J. Membrane Biol. 141, 29–42 (1994)

The Journal of
Membrane
Biology

Hydrochlorothiazide Enhances the Apical Cl^- Backflux in Rabbit Gallbladder Epithelium: Radiochemical Analysis

D. Cremaschi, C. Porta

Dipartimento di Fisiologia e Biochimica Generali, Sezione di Fisiologia Generale, Università degli Studi di Milano, I-20133 Milan, Italy

Received: 29 July 1993/Revised: 5 January 1994

Abstract. Hydrochlorothiazide (HCTZ) was shown to inhibit the transepithelial NaCl transport and the apical Na^+-Cl^- symport and to depolarize the apical membrane potential in the rabbit gallbladder epithelium. The depolarization was likely related to the opening of a Cl^- conductance. To better understand whether an apical Cl^- leak is involved in the mechanism of action of HCTZ, the transapical Cl^- backflux was measured radiochemically by the washout technique. The gallbladder wall, pretreated with pronase on the serosal side to homogenize the subepithelium, was loaded with $^{36}Cl^-$ on the luminal side; mucosal and serosal $^{36}Cl^-$ effluxes (J_m, J_s) were then measured every 2 min. The pretreatment with pronase did not alter the membrane potentials and the selectivity of the epithelium. Under control conditions and the tissue in steady-state, J_m and J_s time courses were each described by two exponential decays (*A*, *B*); the rate constants, k^A and k^B, were 0.71 ± 0.03 and 0.16 ± 0.01 min^{-1}, respectively, and correspondingly the half-times ($t^A_{1/2}$, $t^B_{1/2}$) were 1.01 ± 0.05 and 5.00 ± 0.44 min ($n = 10$); these parameters were not significantly different for J_m and J_s time courses. J_s was always greater than J_m ($J_s/J_m = 2.02 \pm 0.22$ and 1.43 ± 0.17 for *A* and *B* decays). Under SCN^- treatment in steady-state conditions, both J_m and J_s time courses were described by only one exponential decay, the component *B* being abolished. Moreover $t^A_{1/2}$ was similar to that predictable for the subepithelium. It follows that it is the component *B* which exits the epithelial compartment. Based on the intracellular specific activity and $^{36}Cl^-$ J^B_m at 0 min time of the washout experiment, the cell-lumen Cl^- backflux in steady-state was calculated to be equal to about 2 μmol $cm^{-2}hr^{-1}$, in agreement with the value indirectly computable by other techniques. The experimental model was well responsive to different external challenges (increases in media osmolalities; luminal treatment with nystatin). HCTZ ($2.5 \cdot 10^{-4}$ M) largely increased $^{36}Cl^-$ J^B_m. The increase was abolished by luminal treatment with 10^{-4} M SITS, which not only brought back the efflux time courses to the ones observed under control conditions but even increased J_s/J_m of the cellular component, an indication of a reduced J^B_m. It is concluded that HCTZ opens an apical, SITS-sensitive Cl^- leak, which contributes to dissipate the intracellular Cl^- accumulation and to inhibit the NaCl transepithelial transport. Moreover, the drug is likely to reduce the basal electroneutral Cl^- backflux supported by Na^+-Cl^- cotransport, in agreement with the inhibition of the cotransport itself.

Key words: Na^+-Cl^- cotransport — Cl^- pathways — SITS — SCN^- — Nystatin — Washout technique

Introduction

In the epithelium of rabbit gallbladder the neutral entry of NaCl through the apical membrane is sustained by a Na^+/H^+,Cl^-/HCO_3^- double exchange and a hydrochlorothiazide (HCTZ)-sensitive Na^+-Cl^- symport, which are likely to operate in parallel (Cremaschi et al., 1983, 1987*a*, *b*, 1992; Meyer et al., 1990). In the absence of exogenous bicarbonate, with the endogenous bicarbonate made negligible by bubbling 100% O_2 in the bathing salines and possibly, but not necessarily, in the presence of acetazolamide, only the symport is active (Cremaschi et al., 1987*a*, *b*). It can be inhibited by HCTZ, but not by stilbenes, furosemide or bumetanide, and is insensitive to K^+ (Cremaschi et al., 1987*a*, *b*, 1992; Meyer et al., 1990); thereby it is similar to the symport detected in fish urinary bladder and mammal distal tubule rather than to the one observed in the thick

Correspondence to: D. Cremaschi

ascending limb of the Henle loop (Costanzo & Windhager, 1978; Duffey & Frizzell, 1984; Stokes, 1984; Velasquez, Good & Wright, 1984; Eveloff & Warnock, 1987).

In the fish urinary bladder HCTZ inhibits the net transepithelial flux of NaCl and both the transcellular unidirectional fluxes (mucosa-serosa, serosa-mucosa) (Stokes, 1984, 1988). In the rabbit gallbladder on HCTZ treatment the net transepithelial flux of NaCl and the transapical lumen-cell Cl^- influx, sustained by the symport, are both inhibited. Moreover, intracellular Cl^- activity and accumulation are largely reduced (Cremaschi et al., 1992). In parallel, an apical depolarization is elicited which preliminary experiments have shown to be related to the opening of an apical conductive Cl^- leak (Cremaschi et al., 1992, 1993); this side action, absent in the fish urinary bladder, may contribute to dissipating the intracellular Cl^- accumulation in the gallbladder with an electrodiffusive Cl^- backflux to the lumen. To gain a better understanding of the mechanism of action of HCTZ in this epithelium, it is then important to measure the overall transapical unidirectional Cl^- backflux (cell-lumen). This flux is likely to be inhibited in its component sustained by the symport (like in the urinary bladder), but on the whole may be enhanced by the opening of the apical Cl^- leak.

The Cl^- backflux was measured radiochemically by the washout technique, after luminal loading of the isolated tissue with $^{36}Cl^-$. The epithelial component of the luminal efflux was discriminated from the subepithelial component by compartment analysis under steady-state conditions. All the experiments have been conducted in the absence of bicarbonate in the bathing salines so as to eliminate transports due to the double ion exchange component.

Materials and Methods

New Zealand male rabbits (body weight 3–3.5 Kg), kept for 15 days at constant conditions of light/dark and temperature and fed with standard pellets, were killed by cervical dislocation. The excised gallbladders were washed free of bile with saline.

Washout Experiments

The organ was everted, cannulated, filled with 0.2 ml Krebs-Henseleit saline, containing 0.1 mg/ml pronase (type XIV, no. P5147, Sigma Chemical, St. Louis, MO), and dipped in Krebs-Henseleit saline, bubbled with 95% O_2 + 5% CO_2; incubation was prolonged for 20 min at 37°C (temperature chosen to optimize the enzyme action). Finally, the pronase-containing saline was removed, the preparation washed and opened lengthwise; the gallbladder sheet was mounted between two Lucite frames (window: 0.67 cm^2) and clamped between two Lucite chambers with volumes equal to 1 ml (mucosal chamber) and 10 ml (serosal chamber). The tissue was allowed to recover functionality for 30 min at 27°C in phosphate saline. The saline was then renewed and the tissue loaded with $^{36}Cl^-$ on the mucosal side (12 μCi/ml) for 15 min. The large serosal fluid volume allowed radioactivity to remain very low on this side, so as to minimize loading of the subepithelial layers with $^{36}Cl^-$. Finally, the two bathing salines were withdrawn, the tissue was washed three times on both sides with phosphate saline, and the two frames were rapidly removed with the tissue and clamped between new Lucite chambers of equal volume. The chambers were both filled with 2.5 ml phosphate saline which was renewed 10 times every 2 min with the aid of a saline dispenser and a vacuum pump. The dead-time for all the operations occurring between the end of the loading and the washout start was about 30 sec. During the loading and washout period, salines were kept at 27°C, a temperature that allowed the tissue to remain in steady-state for a long time. Samples obtained for each 2 min period were counted for radioactivity with a Minaxi-Tricarb/counter (Packard Instr., Zurich, Switzerland).

Measurement of the Paracellular Cl^- Uptake

The general procedure was the one previously reported (Cremaschi et al., 1992) and the protocol similar to that described for washout determinations: (i) serosal incubation of everted sacs without the enzyme (controls) or with pronase (Krebs-Henseleit bathing saline, at 37°C for 20 min); (ii) incubation of the opened gallbladders for 60 min at 27°C (phosphate saline); (iii) measurement of Cl^- uptake for 45 sec, with $^{36}Cl^-$, ^{3}H-sucrose and 25 mM SCN^- in the luminal phosphate saline. SCN^- was added to abolish the cellular component of the uptake (Cremaschi et al., 1992), so as to measure only the paracellular fraction.

Transmural Cl^- Flux Determinations

The everted gallbladder was treated with pronase at 37°C for 20 min (Krebs-Henseleit saline); then washed, opened lengthwise and mounted (window: 0.67 cm^2) between two Lucite chambers, each filled with 5 ml phosphate saline at 27 ± 1°C, with $^{36}Cl^-$ present (0.5 μCi/ml) in the serosal chamber. After 15 min, the mucosal fluid was renewed and the procedure was repeated every 15 min for 10 experiment periods. Samples of the serosal fluid (0.1 ml), taken every 30 min, allowed the time course of the serosal activity to be checked: it remained constant throughout the experiment.

Electrophysiological Measurements

The set-up procedures for cell membrane potential recordings were similar to those previously described (Cremaschi et al., 1992). Briefly, the shank of the microelectrode, filled with 0.5 M KCl, was connected through a high impedance electrometer (model FD223, World Precision Instruments, New Haven, CT) to a strip chart recorder (PM 8262 Xt Recorder, Philips, Eindhoven, The Netherlands). Short pulses of direct current (20 μA, 200 msec) were passed through the exposed tissue (0.17 cm^2) to check the microelectrode entrance into the cell from the voltage deflections. Criteria for impalement validation were those previously reported (Cremaschi et al., 1992).

Transmural diffusion potentials were measured in phosphate saline by substituting mannitol for all the luminal NaCl.

Histological Preparations

Control tissues and tissues treated with pronase on the serosal side were fixed in Bouin saline, included in paraffin, cut into 10 μm thick sections and stained with hematoxylin-eosine.

SALINES

The composition of the Krebs-Henseleit saline was as follows (mM): 142.9 Na^+, 5.9 K^+, 127.7 Cl^-, 24.9 HCO_3^-, 1.2 Mg^{2+}, 1.2 SO_4^{2-}, 1.2 $H_2PO_4^-$, 2.5 Ca^{2+}; pH 7.4. The phosphate saline contained (mM): 145.3 Na^+, 6.1 K^+, 2.5 Ca^{2+}, 1.2 Mg^{2+}, 125.3 Cl^-, 13.7 SO_4^{2-}, 12.5 mannitol, 2.7 HPO_4^{2-}, 0.7 $H_2PO_4^-$; pH 7.4. Inhibitors were added directly to the solution (since the change in osmolality was negligible) with the exception of SCN^- (25 mM) which was substituted for 12.5 mM SO_4^{2-} and mannitol. HCTZ was dissolved directly in the saline by stirring for 150 min at 24 ± 1°C; the final concentration was checked with a spectrophotometer (Lambda 5, Perkin Elmer, Norwalk, CT) at the wavelength of 226 nm. The salines were bubbled with 95% O_2 + 5% CO_2 (Krebs-Henseleit saline) or 100% O_2 (phosphate saline).

MATERIALS

SITS, HCTZ and nystatin were purchased from Sigma (St. Louis, MO), SCN^- from C. Erba (Milan, Italy).

DATA HANDLING AND STATISTICS

The 2 min effluxes smaller than 2σ of the background (<6 cpm) were discarded as unreliable. Effluxes were then expressed as mean rate during each 2 min measurement period (cpm min^{-1}). The time-courses of the tissue-lumen (J_m) and tissue-serosa (J_s) effluxes were analyzed in each experiment looking at the best fits for an exponential decay in the forms:

$y = A \cdot \exp(-kx)$ or $y = A \cdot \exp(-kx) + B \cdot \exp(-k'x)$ or for a mixed exponential $y = A \cdot \exp(-kx) + B \cdot [1 - \exp(-k'x)]$

(goodness of fit assessed using relative distances). The parameters calculated in this way, experiment by experiment, were then averaged and statistically compared. When possible, paired-data *t*-test (one tail or two tails) was used; otherwise, we used the unpaired data *t*-test. In the figures, the logarithms of the mean effluxes of many experiments are plotted against time to show indicatively the result obtained in each experimental condition. The straight lines in Figs. 2*b* and 3 were calculated from the exponential curves obtained from the best fit of the corresponding mean efflux time courses. No statistical analysis was performed on these averaged time courses.

THEORETICAL CONSIDERATIONS

To appreciate the experimental approach and the results obtained, two main points must be emphasized first. (i) If the tissue is in steady-state, on loading with $^{36}Cl^-$ from the lumen, the equations that describe the subsequent mucosal and serosal $^{36}Cl^-$ unloadings represent more or less complex exponential decays. This is independent of the transport mechanisms involved and their driving forces, inasmuch as the concentration in the tissue and the fluxes of the nonradioactive Cl^- are constant. It is only the labeling of the tissue pools, transport sites and fluxes which decreases, driven only by the differences in specific activity between the tissue and the external media. Moreover, the two $^{36}Cl^-$ effluxes toward the serosal and mucosal medium at any moment continue to label and represent the corresponding steady non-radioactive effluxes, although with specific activity decreasing with time (Kotyk & Janacek, 1970; Jacquez, 1972). (ii) If the tissue is made by a single compartment facing both the mucosal and serosal medium, the same pool of $^{36}Cl^-$ feeds both exits. In this case the time courses of the two effluxes are predicted to be described by two simple exponential decays with equal rate constants:

$$J_s = J_{s,o} - \exp(kt) \quad (1)$$

$$J_m = J_{m,o} - \exp(kt) \quad (2)$$

where J_s and J_m are the tissue-serosal and the tissue-mucosal medium effluxes, respectively; t is time; k is the rate constant of unloading from the compartment; $J_{s,o}$ and $J_{m,o}$ are the two effluxes at $t = 0$ min (*see* Appendix).

Consequently, the time courses of the Briggsian logarithms of the two effluxes are described by two parallel straight lines. Moreover, the efflux ratio J_s/J_m is equal to $J_{s,o}/J_{m,o}$ and constant throughout the washout experiment. It is independent of the $^{36}Cl^-$ loading in the compartment.

Results

THE TREATMENT WITH PRONASE

The epithelium of the rabbit gallbladder (25–30 μm tall, highly folded) lies on a subepithelium (about 550 μm thick), made by a corion, two layers of smooth muscle cells (with an interposed connective layer containing large capillaries) and a mesothelium (Fig. 1*a*). The organization of the epithelium was apparently not affected by the serosal treatment with pronase (0.1 mg/ml), whereas all the subepithelial structures were dissegregated and any clear distinction in orderly layers disappeared (Fig. 1*b*).

The apical membrane potential of the epithelial cells (V_m) can be taken as an index of the viability degree and of the steady-state of the epithelium, as it appeared stable for at least 90 min after tissue isolation (Cremaschi et al., 1992). With the tissue incubated for 50 min in phosphate saline (control), V_m was −66.1 ± 0.5 mV (127 cells). On treatment with pronase for 20 min and incubation in phosphate saline for 30 min, V_m was not significantly different (−64.8 ± 0.8 mV, 51 cells).

The epithelium also seemed to maintain its viability as a diffusional barrier. In fact, the serosal specific activity, at the end of the 15 min luminal loading with $^{36}Cl^-$, was only 0.6 ± 0.1% of the mucosal activity in spite of the previous exposure to pronase (n = 12). This point was better investigated by measuring paracellular Cl^- uptakes. They turned out to be 2.7 ± 0.6 and 3.2 ± 0.8 μmol $cm^{-2}hr^{-1}$ under control conditions and on treatment with pronase, respectively (n = 9 in either condition). The difference is not significant; moreover, both values are even lower than those we have generally measured under control conditions (5–6 μmol $cm^{-2}hr^{-1}$, Cremaschi et al., 1992). Finally, the transmural serosa-mucosa $^{36}Cl^-$ fluxes on treatment with pronase were steady within 15 min after $^{36}Cl^-$ addition, for at least 135 min (*data not shown*).

All these data demonstrate that the epithelium (cells and junctions) are viable and steady for a long time after isolation and treatment with the enzyme.

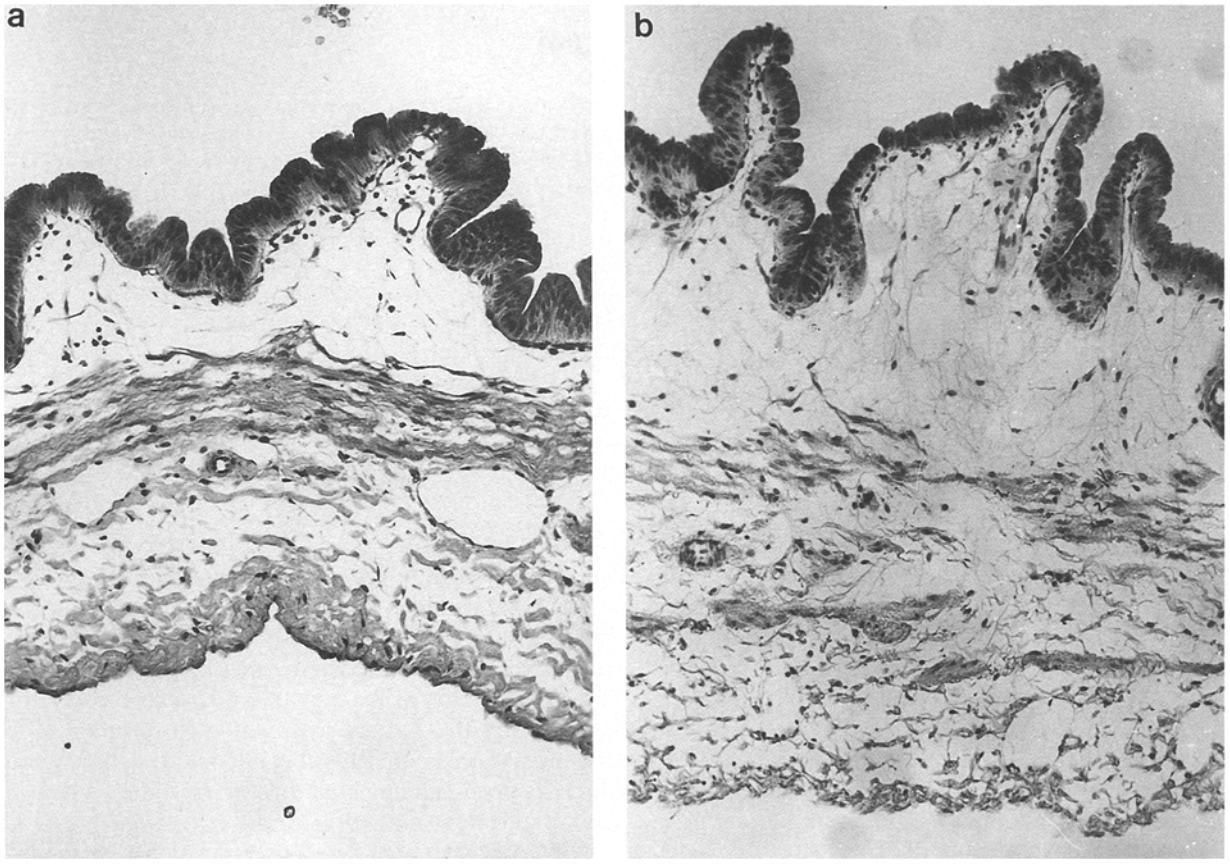

Fig. 1. Histological sections of rabbit gallbladder (magnification: 200×). (*a*) Control, (*b*) after treatment with pronase.

THE $^{36}Cl^-$ EFFLUXES (TISSUE IN STEADY-STATE)

The serosal and mucosal effluxes of $^{36}Cl^-$, (J_s, J_m; cpm min^{-1}), obtained by time-averaged means of 10 experiments, were plotted against time in a semilogarithmic scale (Fig. 2*a*) to exemplify the result. At first sight, it is evident that the data points are not interpolated by two parallel straight lines, but by two curves, with the result that more than one compartment seems to be involved (*see* Theoretical Considerations). Moreover, the two curves, roughly parallel for about 10 min, then tend to approach. Actually, the measured J_s/J_m ratios, averaged during each experiment period, progressively decrease (decrease highly significant 12 min after the washout start, Table 1). The ratio is significantly greater than 1 at any period.

If the time courses of the two effluxes are analyzed in each experiment, the best fit is obtained with two exponential decays, each one in the following form

$$J_s = J^A_{s,o} \cdot \exp(-k^A_s t) + J^B_{s,o} \cdot \exp(-k^B_s t) \quad (3)$$

$$J_m = J^A_{m,o} \cdot \exp(-k^A_m t) + J^B_{m,o} \cdot \exp(-k^B_m t) \quad (4)$$

with the corresponding rate constants nearly equal in the two equations ($k^A_s \simeq k^A_m$, $k^B_s \simeq k^B_m$), and $J^A_{s,o}$ and $J^B_{s,o}$ larger than $J^A_{m,o}$ and $J^B_{m,o}$ respectively; $r^2 = 1$ in each fit. The results reported in Table 2 are obtained by averaging the parameter values calculated from the analysis of each experiment. Actually, they show that the corresponding rate constants are not significantly different in the two equations so that it is possible to average k^A_m, k^A_s into only k^A (=0.71 min^{-1}) and k^B_m, k^B_s into only k^B (0.16 min^{-1}). The corresponding averaged half-times are: $t^A_{1/2} = 1.01$ min and $t^B_{1/2} = 5.00$ min. Based on these data, the following equations can be set up to express the time courses of the two effluxes:

$$J_s = 1{,}966 \cdot \exp(-0.71t) + 103 \cdot \exp(-0.16t) \quad (5)$$

$$J_m = 998 \cdot \exp(-0.71t) + 66 \cdot \exp(-0.16t) \quad (6)$$

Thus, each time course displays two phases (*A*, *B*) in the exponential decay, the first faster than the second (different rate constants and half-times, $P < 0.01$). Since each phase has equal rate constants for J_s and J_m, in semilogarithmic scale (Fig. 2*b*), two parallel straight lines describe J_s and J_m time courses during the slow phase (main figure) and, equally, during the fast phase (inset). The calculated J_s/J_m ratio is different ($P <$

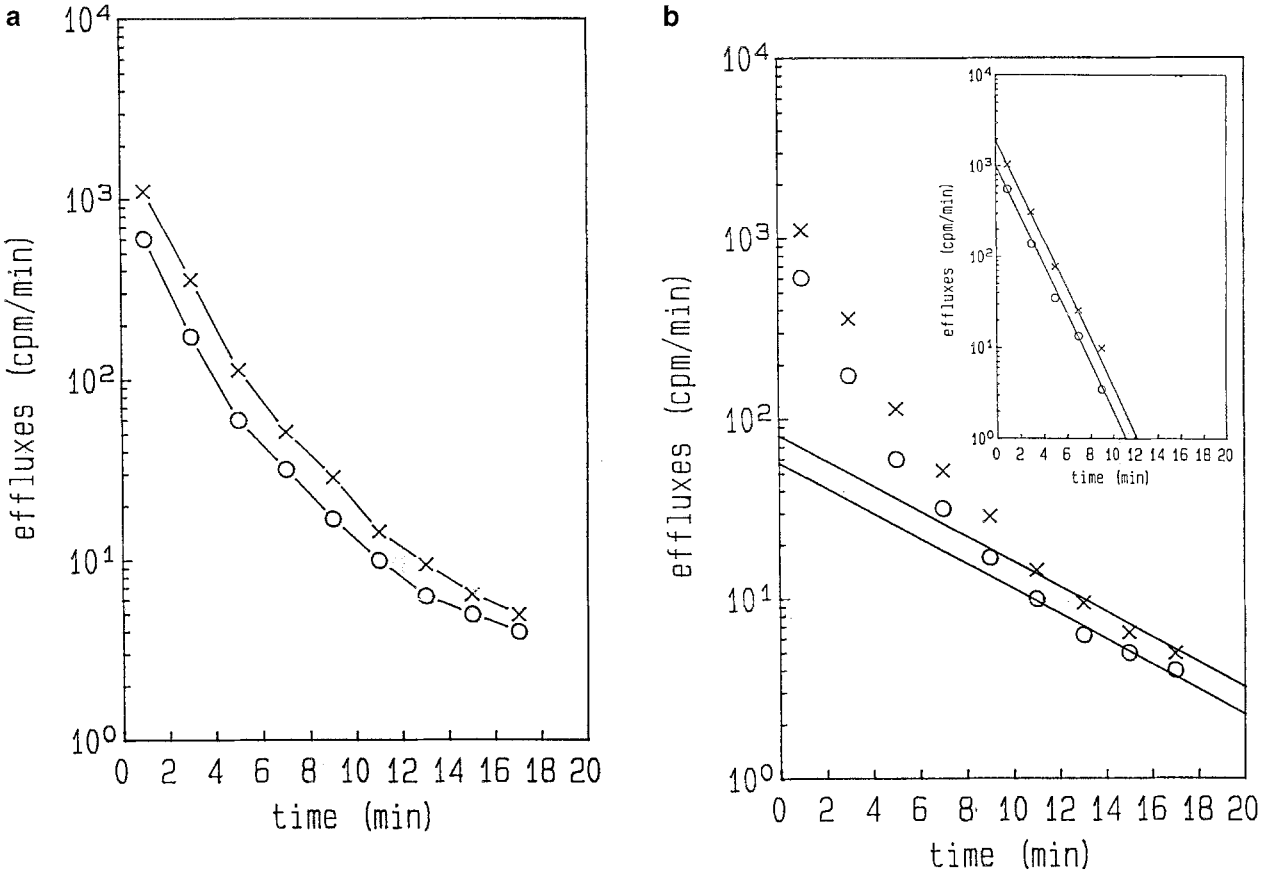

Fig. 2. (*a*) Time courses of the effluxes from the tissue to the mucosal or serosal medium (J_m, J_s) under control conditions (tissue in steady-state conditions; $n = 10$). Effluxes measured every 2 min and expressed as cpm min^{-1}. (O) J_m; (X) J_s. (*b*) Analysis of the time courses of the effluxes reported in *a*. The best fitting of the mean data points of the 10 experiments is obtained with the sum of two exponential decays for each time course (nonlogarithmic scale; $r^2 = 1$ for each timecourse). The two straight lines corresponding in semi-logarithmic scale to the pair of exponential curves with slower decay (main figure) or with faster decay (inset) are parallel. The data points reported in the inset, well interpolated by the straight lines, are calculated from the difference between the experimental points in the main figure and the corresponding extrapolated points lying on the two straight lines representing the slow decay.

0.05) in the fast and the slow phase, the former (2.03) being greater than the latter (1.43), though both significantly greater than 1 (Table 2). This accounts for the decrease in the experimental ratio with time (Table 1).

All these findings indicate that two parallel compartments, A and B unload $^{36}Cl^-$, each one into both the serosal and the mucosal medium, the *A* compartment with higher rates; for both compartments, unloading to the serosal side is greater.

Based on the integration of the exponential decays reported above for J_s and J_m, defined between time equal to 0 and 50 min, it is possible to calculate the $^{36}Cl^-$ initial loading for the A and B compartments. Table 3 shows that A loading is significantly larger, B loading being about 17% of the total. However, it is also easy to calculate that 4 min after the beginning of unloading, compartment A has lost 94.3% of its load, whereas compartment B only 47.7% with the result that residual loading of B now dominates (70% of the total).

Treatment with SCN^- (Tissue in Steady-State)

To check whether one of the two components of the effluxes is related to epithelium, both tissue sides were maintained treated with 25 mM SCN^- during the loading and washout periods. It is known that in a few seconds SCN^- totally abolishes the apical Cl^- entry into the gallbladder epithelial cells (Cremaschi, Hénin & Meyer, 1979; Cremaschi et al., 1983, 1987*b*). This should largely reduce or even eliminate loading of the epithelial compartment and modify the efflux time course. Figure 3 exemplifies the result by reporting the mean effluxes obtained ($n = 11$): actually, under these conditions the two efflux time courses are singled out by only one pair of parallel straight lines; accordingly, the experimental J_s/J_m ratio is not significantly different at any period (Table 1). Thus, only one of the two compartments observed under control conditions remains effective on treatment with SCN^-.

Table 1. Efflux ratios (J_s/J_m), averaged every four minutes, measured under different conditions

Experimental conditions	n	J_i/J_m (min)				
		0–4	4–8	8–12	12–16	16–20
Control	10	1.93 ± 0.10	1.84 ± 0.14	1.68 ± 0.15	1.43 ± 0.10	
		**	**	**	**	
			NS	MS	****	
SCN^-	11	2.57 ± 0.18	2.62 ± 0.15	2.25 ± 0.14		
		**	**	**		
			NS	NS		
Sucrose (mucosal side)	5	1.67 ± 0.28	1.42 ± 0.29	0.98 ± 0.14	0.84 ± 0.12	1.01 ± 0.10
		*	NS	NS	NS	NS
			NS	****	****	****
Sucrose (serosal side)	3	1.73 ± 0.26	2.47 ± 0.21	2.04 ± 0.38	1.80 ± 0.35	
		*	**	*	*	
			***	NS	NS	
Nystatin	6	1.82 ± 0.13	0.95 ± 0.13	1.03 ± 0.16	1.04 ± 0.12	
		**	NS	NS	NS	
			****	****	****	
HCTZ	5	1.72 ± 0.08	1.17 ± 0.10	1.10 ± 0.17	0.87 ± 0.14	0.86 ± 0.16
		**	NS	NS	NS	NS
			****	****	****	****
HCTZ + SITS	4	1.82 ± 0.08	1.86 ± 0.17	1.71 ± 0.10	1.74 ± 0.22	
		**	**	**	**	
			NS	NS	NS	

* $P < 0.05$. ** $P < 0.01$ (compared with 1). *** $P < 0.05$. **** $P < 0.01$ (compared with J_s/J_m at 0–4 min). NS, not significant; MS, marginally significant ($P < 0.07$).

Table 2. Time course analysis of the $^{36}Cl^-$ effluxes from the tissue to the mucosal or serosal medium (J_m, J_s), under control conditions or conditions of treatment with SCN^-

	Control		SCN^- treatment	P	
	A	B		*vs.* A	*vs.* B
$J_{m,o}$ (cpm min^{-1})	998 ± 146	66 ± 21	404 ± 36	*****	*****
$J_{s,o}$ (cpm min^{-1})	1,966 ± 318*	103 ± 39	1,071 ± 150	****	*****
k_m (min^{-1})	0.73 ± 0.04	0.16 ± 0.02	0.46 ± 0.04	*****	*****
k_s (min^{-1})	0.69 ± 0.05	0.16 ± 0.02	0.47 ± 0.04	*****	*****
k (min^{-1})	0.71 ± 0.03	0.16 ± 0.01	0.46 ± 0.03	*****	*****
$t_{1/2}$ (min^{-1})	1.01 ± 0.05	5.00 ± 0.44	1.57 ± 0.07	*****	*****
J_s/J_m	2.03 ± 0.22***	1.43 ± 0.17**	2.70 ± 0.29***	NS	*****

Effluxes at 0 min time ($J_{m,o}$, $J_{s,o}$), rate constants (k_m, k_s), averaged k_m and k_s (k), averaged half-times ($t_{1/2}$) and efflux ratio (J_s/J_m) for the apparent compartments A and B. Controls: $n = 10$. SCN^- treatment: $n = 11$. * $P < 0.01$ (compared to the corresponding m parameter). ** $P < 0.05$. *** $P < 0.01$ (compared to 1). **** $P < 0.05$. ***** $P < 0.01$ (compared to controls A or B).

Correspondingly, the analysis on single experiments gives better fittings with only one exponential for each time course ($r^2 = 1$ in any case; parameters reported in Table 2). Since in this case too k_m and k_s are not significantly different, a sole k (0.46 min^{-1}) can be calculated as equal for the two efflux time courses. Based on this, the following two exponential equations can be set up to express J_s and J_m against time (t):

$$J_s = 1{,}071 \cdot \exp(-0.46t) \quad (7)$$

$$J_m = 404 \cdot \exp(-0.46t) \quad (8)$$

The k value and the corresponding $t_{1/2}$ (1.57 min) are intermediate between the corresponding values calculated for the A and B components in control conditions and significantly different from both of them. However, $t_{1/2}$ is much more similar to the A component (1.57 *vs.* 1.01, compared to 5.00 min). The J_s/J_m ratio (2.70) is not significantly different from that of component A, but is significantly higher than that of B. The loading (Table 3) is significantly reduced compared to the total loading measured under control conditions, as expected if only one of the two compartments has been loaded.

Table 3. $^{36}Cl^-$ loading (cpm) in the whole tissue (T) or in the parallel A and B compartments

	Control			(B/T) · 100	SCN^- treatment (cpm)
	T (cpm)	A (cpm)	B (cpm)		
Loading	5,439 ± 914	4,535 ± 776**	904 ± 216***	16.6 ± 3.2***	3,278 ± 435*, ns, ****

* $P < 0.05$, ** $P < 0.01$ (compared to the T loading). *** $P < 0.01$ (compared to 0). **** $P < 0.01$ (compared to control B). NS, not significantly different (compared to control A).

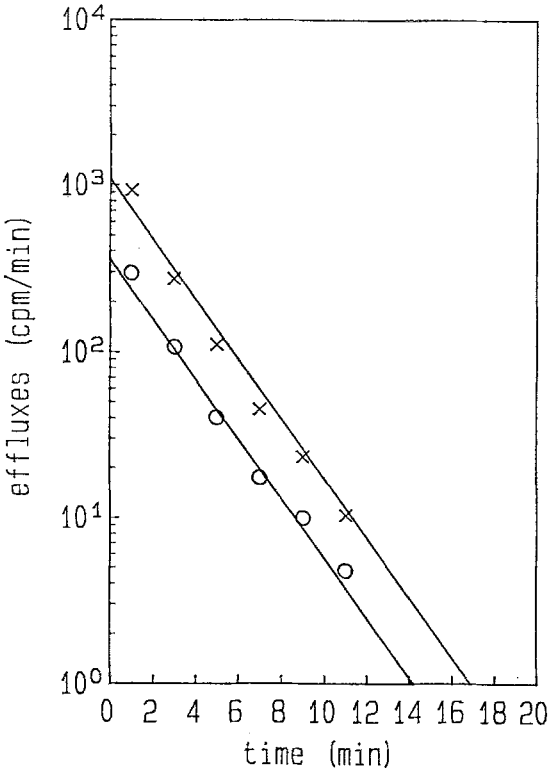

Fig. 3. Time courses of the effluxes from the tissue to the mucosal or serosal medium (J_m, J_s) under SCN^- treatment (tissue in steady-state conditions; $n = 11$). The straight lines shown represent the best fitting of the mean data points. The tissue was treated with 25 mM SCN^- on both sides during the loading and washout periods. (O) J_m; (X) J_s.

It is not significantly different from that of compartment A, but nearly four times larger than that of B.

These results indicate that it is compartment B which has been kept unloaded in the presence of SCN^- and which thus corresponds to the epithelial cells.[1]

[1] The similar but significantly higher $t_{1/2}$, observed under SCN^- treatment, compared to the $t_{1/2}$ of compartment A measured under control conditions, cannot be simply explained by the closure of the cell pathway operated by SCN^-. In fact, the backflux from the subepithelial layer to the mucosal medium does not cross the cells even under control conditions (Cremaschi & Hénin, 1975). It is due to a reduction in permeability of the leaky-junction pathway, elicited in a few minutes by SCN^- and lasting for at least half an hour, that is for the whole loading and unloading period (*unpublished results*).

Perturbation of Tissue Steady-State

Since HCTZ should challenge the tissue steady-state by operating on the mucosal side, we checked the J_m and J_s responsiveness by increasing the luminal osmolality or treating luminally with nystatin, a polyene antibiotic forming pores in the plasma membranes.

By adding 100 mM sucrose to the luminal medium 4 min after the washout start (when cellular load is dominant), the sweeping away effect, so caused towards the lumen, should decrease the J_s/J_m ratio. As expected, the efflux asymmetry is rapidly reduced and even tends to be inverted (Fig. 4*a*, $n = 5$); the J_s/J_m ratio (Table 1), from a value significantly higher than 1 (1.67) during the control period, decreases to values even tending to be lower than 1 (0.84). The significant ($P < 0.01$) final increase to 1.01 is probably due to a time-dependent decrease of the osmolality gradient, related to the asymmetric subepithelial unstirred layer (Wright, Smulders & Tormey, 1972).

As a countercheck, in three experiments 100 mM sucrose was added to the serosal medium. In this case, the osmotic gradient should increase the J_s/J_m ratio by a sweeping away effect toward the serosa. Figure 4*b* shows that the efflux asymmetry is rapidly enhanced. J_s/J_m ratio (Table 1) increases significantly from 1.73 to 2.47; then, although decreasing with time, probably due to the progressive dissipation of the osmotic gradient (*see above*), it always remains significantly higher than 1.

In six experiments, again 4 min after the washout start, nystatin was added to the luminal medium (30 μg/ml = 169.2 U/ml). Figure 5 shows J_m to increase rapidly to such an extent that the efflux asymmetry is abolished and even inverted. The efflux ratio (Table 1) decreases significantly from the value of 1.82 (control period) to values of around 1 for all the following periods.

The Effects of Hydrochlorothiazide

Figure 6 reports the mean J_m and J_s time courses obtained before and after luminal treatment with $2.5 \cdot 10^{-4}$ M HCTZ ($n = 5$). The mucosal efflux increases and in 2 min becomes nearly equal to the serosal one to overcome it after 8–10 min of treatment. The efflux ratio, significantly different from 1 during the control period

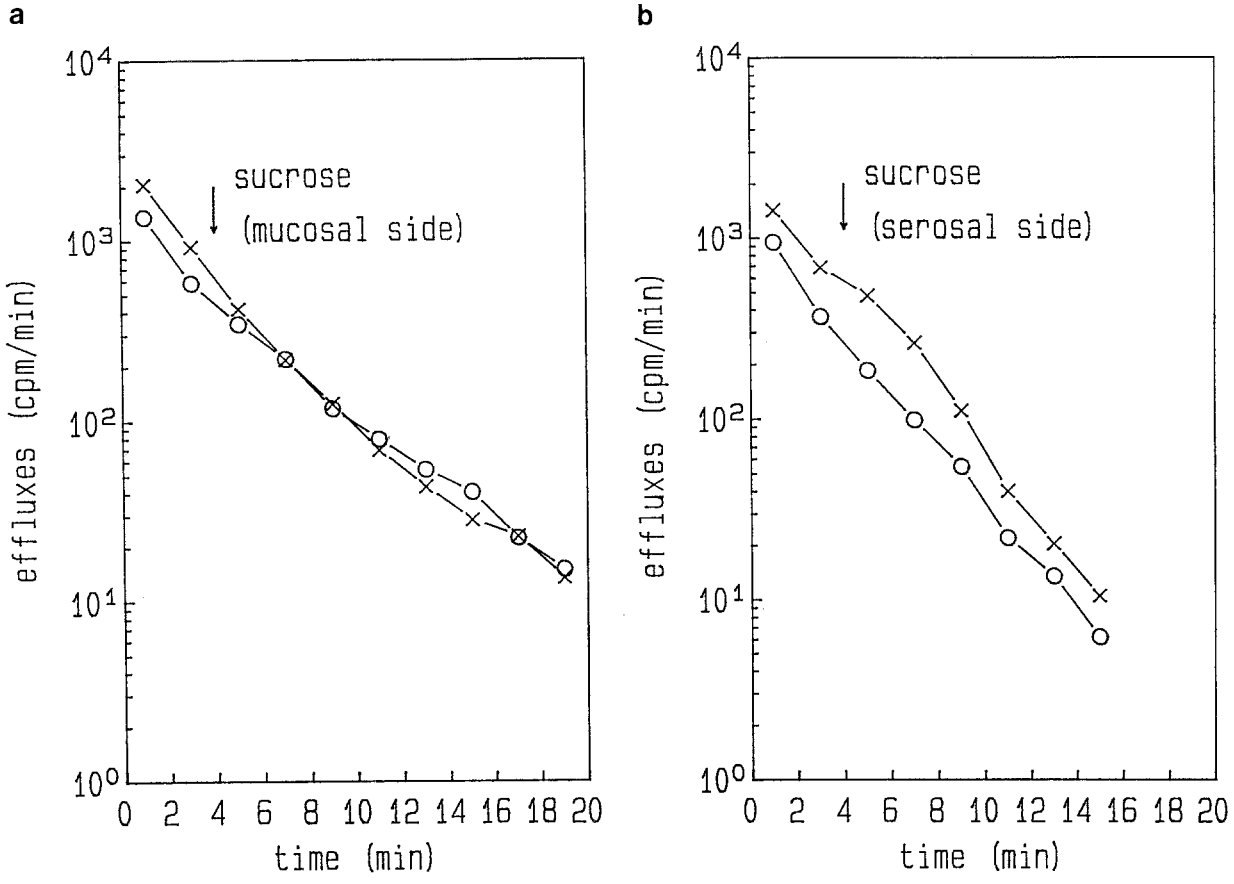

Fig. 4. Time courses of the effluxes from the tissue to the mucosal or serosal medium (J_m, J_s): an osmotic gradient was imposed 4 min after the beginning of the washout experiment (tissue in nonsteady-state conditions) by addition of 100 mM sucrose to the mucosal (*a*) or the serosal (*b*) medium. Each point value represents the mean of 5 (*a*) or 3 (*b*) experiments. (O) J_m; (X) J_s.

(1.72), drops significantly to 1.17 in the first 4 min of treatment and then tends to decline with time to below 1 (Table 1). The result is roughly similar to that obtained with nystatin, although maximal effects seem to be reached more slowly. By integrating the apical effluxes from 4 to 20 min with radioactivity, which has exited the tissue apically after HCTZ treatment, proves on the whole to be 2.3 times higher compared to that of the control.

Conversely, if the tissue is concomitantly treated with HCTZ ($2.5 \cdot 10^{-4}$ M) and SITS (10^{-4} M), the effect is completely eliminated (Fig. 7, $n = 4$): the time courses and the efflux ratios for the entire washout period are not significantly different from those observed in control conditions (Figs. 2*a*, 7, Table 1). However, it is noteworthy that the efflux ratio at 12–16 min is not significantly different from its inner control at 0–4 min, whereas in the control experiments a significant decrease is observed (Table 1). Thus, HCTZ-SITS treatment seems to maintain a higher efflux asymmetry at the end of the unloading.

The transmural serosa to mucosa $^{36}Cl^-$ flux was in steady-state in 15 min and remained so under control conditions until the end of the experiment. By luminal treatment with HCTZ (60 min after the experiment start) not only was the efflux not enhanced, but it even decreased by $10.2 \pm 1.2\%$ ($n = 4$) in 15 min ($P < 0.01$) and remained so throughout the whole experiment.

The transmural diffusion potential, measured in phosphate saline by substituting mannitol for all the luminal NaCl, was unaffected by $2.5 \cdot 10^{-4}$ M HCTZ (-16.0 ± 0.6, -16.3 ± 0.6, -16.9 ± 0.7 mV, before, during and after treatment; $n = 10$).

Discussion

Analysis of the Results under Steady-State Conditions

The rabbit gallbladder wall apparently can be schematically represented by two compartments in series, the ep-

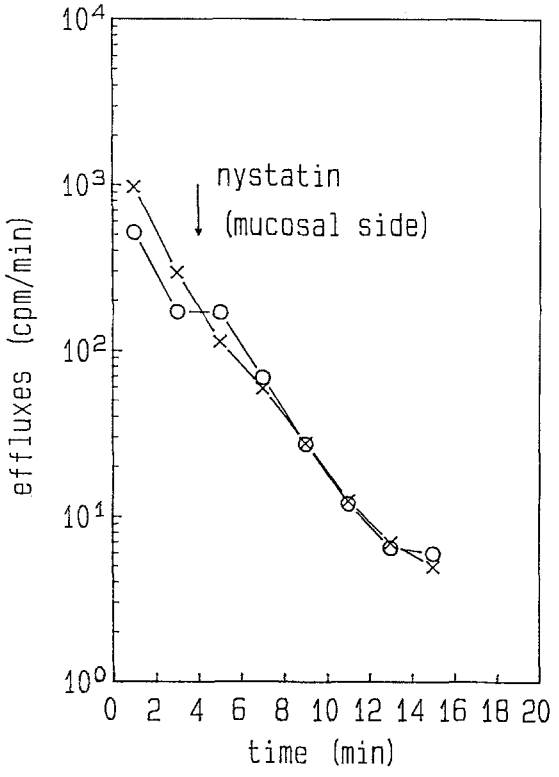

Fig. 5. Time courses of the effluxes from the tissue to the mucosal or serosal medium (J_m, J_s): treatment with nystatin on the mucosal side (30 μg/ml) 4 min after the beginning of the washout experiment (tissue in nonsteady-state conditions; $n = 6$). (O) J_m; (X) J_s.

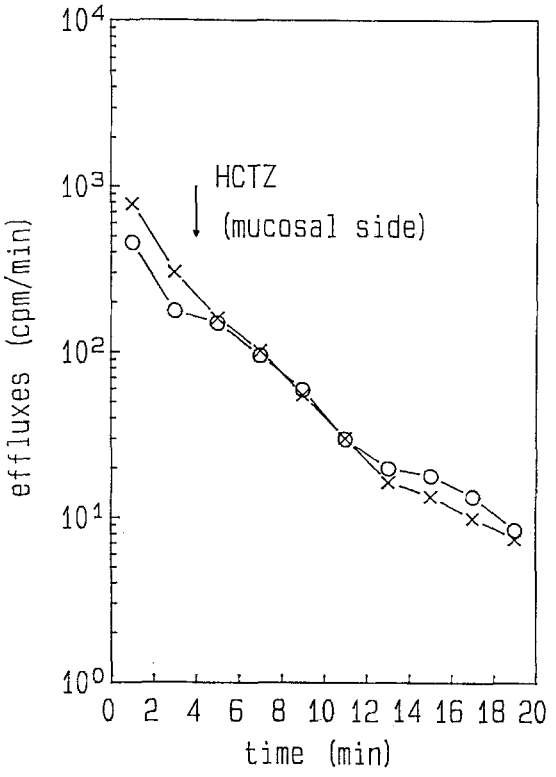

Fig. 6. Time courses of the effluxes from the tissue to the mucosal or serosal medium (J_m, J_s): treatment with $2.5 \cdot 10^{-4}$ M HCTZ on the mucosal side 4 min after the beginning of the washout experiment (tissue in nonsteady-state conditions; $n = 5$). (O) J_m; (X) J_s.

ithelium and the subepithelium, if the adherent unstirred layers of fluid are reduced to a minimum by stirring the bathing salines. Under the conditions, used in this case, of treating the connective tissue with pronase and loading with $^{36}Cl^-$ only on the mucosal side, with a negligible concentration of the isotope achieved in the large serosal medium during the incubation, the subepithelium should be largely dissegregated and homogenized (as in fact occurs) and should be loaded to a minimum. On the other hand, its volume is more than five times larger than that of the epithelium, also taking into account that large foldings increase the epithelial area by 3.8 times (Cremaschi et al., 1987*a*). Moreover, Cl^- activity in the epithelial cell is at least three times lower than that of the external media and less labeled with $^{36}Cl^-$ (lower specific activity achieved) than the loading medium, due to the basolateral $^{36}Cl^-$ leak, even if a steady-state has been reached. Finally, the subepithelial layer receives $^{36}Cl^-$ both from the epithelial cells and through the paracellular pathways. Therefore, loading of the subepithelium can be high in spite of the experimental precautions taken.

We can summarize the results obtained with the tissue in steady-state as follows. (i) The time course of each $^{36}Cl^-$ efflux is described by the sum of two exponential decays (a fast one and a slow one). (ii) In the fast decays, k_m and k_s are equal to each other; the same for the slow decays. Thus, J_m and J_s must be fed by the same single compartment during each phase, but in the two phases by two different and independent compartments, both facing the mucosal and serosal media and thereby paralleling each other. (iii) One (compartment A) is larger than the other (compartment B), with an about 5 times greater loading capacity and a 4–5 times higher unloading rate constant. It has already lost about 94% of its load in the 4 min after the washout start and the loading of the second smaller compartment becomes dominant after this period. (iv) Both compartments display a higher efflux to the serosal medium, but with different J_s/J_m. (v) Treatment with SCN^- (tissue in steady-state) allows identification of the epithelial cell compartment in compartment B, with less loading capacity and slower unloading rate. Therefore, the parallel compartment A must correspond to the subepithelial layer or part of it.

At first sight, the subepithelial layer seems to be in series and not in parallel with the epithelial cells; thus, the last point deserves some comments.

It is well known that the intercellular route in this epithelium is leaky (Frömter & Diamond, 1972; Hénin

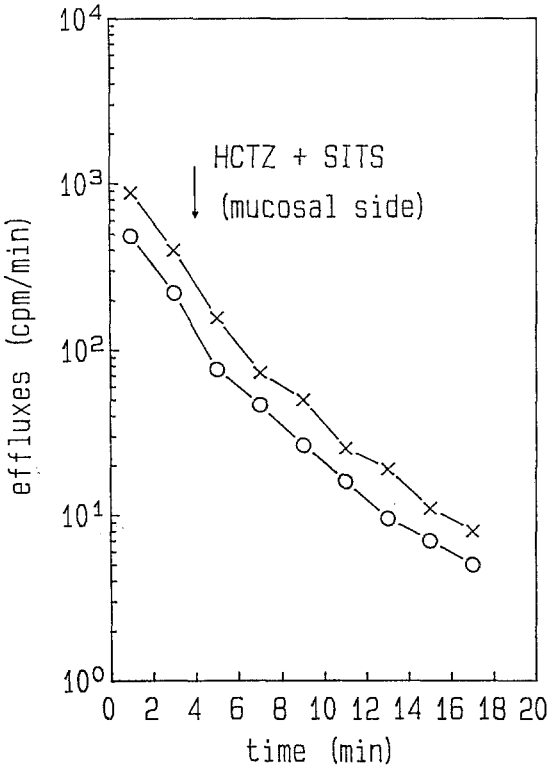

Fig. 7. Time courses of the effluxes from the tissue to the mucosal or serosal medium (J_m, J_s): treatment with $2.5 \cdot 10^{-4}$ M HCTZ and 10^{-4} M SITS on the mucosal side 4 min after the beginning of the washout experiment (tissue in nonsteady-state conditions; $n = 4$). (O) J_m; (X) J_s.

et al., 1977); moreover, $^{36}Cl^-$ does not enter the epithelial cell on the subepithelial side through the basolateral membrane, at least in the absence of bicarbonate in the incubation media (Cremaschi & Hénin, 1975), as occurs in our experimental conditions. Thus, the subepithelial compartment not only unloads directly into the serosal medium which it faces, but also actually unloads directly into the mucosal medium, through a pathway parallel to the epithelial cells (Fig. 8).

The epithelial cells discharge $^{36}Cl^-$ into the lumen through the apical membrane; a second component of the luminal efflux takes place through the lateral membrane into the intercellular channel from where it escapes back into the lumen through the leaky junction, overlapping the efflux coming from the subepithelial compartment. Thus, the epithelial and the subepithelial J_m's are clearly parallel.

The epithelial cells also unload $^{36}Cl^-$ into the serosal medium through the basolateral membranes and, in this case, the unloaded $^{36}Cl^-$ must first cross the subepithelial layer. However, this is generally considered as an unstirred layer rather than a stirred compartment. As such, it behaves like a thick diffusional barrier (and with greater reason on treatment with pronase) which directly interconnects the epithelial cells and the serosal medium (Diamond, 1966; Wedner & Diamond, 1969; Wright et al., 1972). By contrast, for the $^{36}Cl^-$ amount trapped in the subepithelium at the loading period end, this layer behaves as a reservoir which then directly unloads $^{36}Cl^-$ into the serosal and mucosal media as discussed above (Fig. 8).

In conclusion, the epithelial cells and the subepithelial layers behave like two parallel and independent compartments. Some further observations have to be made.

For a compartment open to the serosal medium, but with a diffusional exit to the mucosal side restricted to the leaky junction pathway, the J_s/J_m ratio ($\simeq 2$) of the subepithelial tissue seems rather low. However, if the subepithelium is actually a diffusional barrier, its $^{36}Cl^-$ concentration decreases with the distance from the epithelium. About 90% of $^{36}Cl^-$, at the most, is then trapped in the 370 μm thick layer just beneath the epithelium.[2] It is essentially this layer which behaves as compartment A and the remaining layer (at least 180 μm thick) behaves as a diffusional barrier which limits J_s exit towards the serosal side. This can account for the low J_s/J_m ratio.

Finally, $^{36}Cl^-$ J_m should correctly label and represent the actual, constant Cl^- backflux from the cells. In fact, the progressive decay of $^{36}Cl^-$ efflux corresponds to a proportional decay of the specific activity in the cell. Moreover, the mucosal barrier is only a few μm thick, being set-up (Fig. 8) by the apical plasma membrane, in parallel with the lateral membrane/part of lateral channel length/leaky junction—all in series with the thin, unstirred luminal layer (which can be estimated with ^{3}H-sucrose, a marker of the extracellular apical space, to be about 3 μm, *see* Materials and Methods). Since the mucosal barrier is so thin, the delay between the entry of the efflux into the barrier and its exit to the lumen is negligible, compared to the measuring time of

[2] Let us suppose that, at the end of the loading period, not only the tissue and the nonradioactive fluxes, but also the transmural $^{36}Cl^-$ fluxes and the $^{36}Cl^-$ distribution in the tissue are in steady-state. Then, at time = 0 min of the washout experiment $^{36}Cl^-$ concentration in the subepithelial layer should decay spatially with a linear profile, the maximal concentration being near the epithelium ($x = 0$ μm) and the minimal at the boundary with the stirred serosal saline ($x = \Delta x$). If the latter concentration, equal to that in the serosal medium (0.6% compared to that of the mucosal medium), is considered negligible and if $\Delta x = 550$ μm, then about 90% of the $^{36}Cl^-$ amount, present in the subepithelium at the end of loading, should be in the 370 μm thick layer, closer to the epithelium, independently of the $^{36}Cl^-$ concentration at $x = 0$ μm. If, by contrast, at the end of the loading period the $^{36}Cl^-$ distribution has not achieved steady-state, the $^{36}Cl^-$ concentration profile in the subepithelial layer should display a spatial exponential decay and, thereby, 90% of the $^{36}Cl^-$ present should be contained in a layer even thinner than 370 μm.

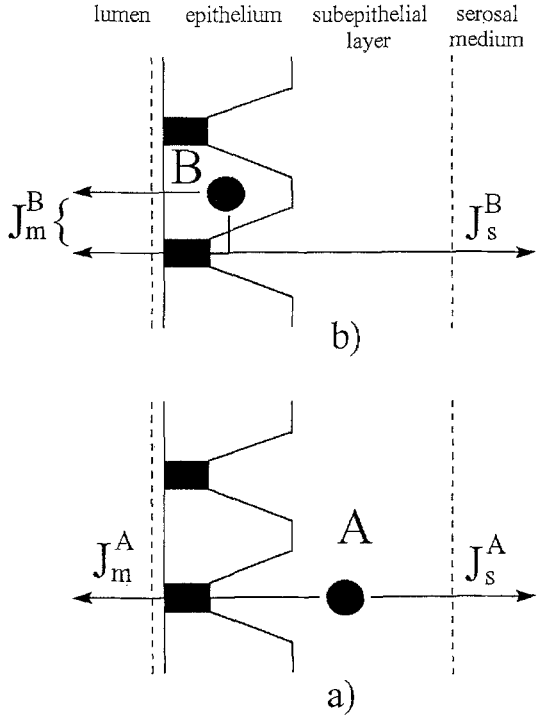

Fig. 8. Schematic layout of the tissue compartments and their unloadings. (*a*) Subepithelial layer (compartment A). (*b*) Epithelial cells (compartment B). J^A_m, J^A_s: Mucosal and serosal effluxes from compartment A. J^B_m, J^B_s: Mucosal and serosal effluxes from compartment B.

2 min, so that the measured efflux to the lumen corresponds well to the efflux leaving the cytoplasm.

By contrast, the very thick, unstirred subepithelial layer, which forms the largest part of the serosal barrier for compartment B, leads to a non-negligible delay between the $^{36}Cl^-$ efflux entry into the barrier from the cytoplasm and its exit into the serosal medium. This can involve an underestimation of the actual serosal Cl^- efflux in steady-state.

The last observation does not impair the compartment analysis reported here and its conclusions. However, it entails that: (i) the actual serosal Cl^- efflux in steady-state cannot be calculated, based on $^{36}Cl^-$ J_s, (ii) the $^{36}Cl^-$ J_s/J_m ratio for compartment B is proportional in each period, but underestimated, compared to the actual Cl^- J_s/J_m ratio in steady-state.

Validation of the Model

Based on the model reported above, some predictions can be made. First, the steady-state Cl^- backflux (J_m) can be calculated, as defined above and in Fig. 8. By knowing the loading of the cellular compartment at time = 0 min (904 cpm, Table 3), the intracellular Cl^- activity (30 mM, Cremaschi et al., 1992), the cell volume (apparently exposed area = 0.67 cm^2; correction factor for the actual area = 3.8; cell height = 28 μm; *see* Cremaschi et al., 1987*a*), the mucosal $^{36}Cl^-$ efflux at 0 min time $J^B_{m,o}$ (=66 cpm min^{-1}, Table 2), a steady-state Cl^- backflux equal to about 2 μmol cm^{-2} hr^{-1} can be calculated. This value fits well with the one which can be calculated knowing that the apical Cl^- influx is about 11 μmol cm^{-2} hr^{-1} (Cremaschi et al., 1992) and the net transepithelial Cl^- flux is about 9 μmol $cm^{-2}hr^{-1}$ (measured on an equivalent flat sheet of gallbladder by an electrical method: Riccardi, Porta, Cremaschi, 1993); thereby, the backflux is clearly equal to about 2 μmol $cm^{-2}hr^{-1}$. Based on the same data, the Cl^- J_s/J_m ratio should be 9/2 = 4.5 against the value of 1.43 reported in Table 2, which is clearly underestimated as predicted (*see above*).

Secondly, it is possible to estimate roughly the half-time of the subepithelial unloading from the formula (Diamond, 1966): $t_{1/2} = 0.38 \cdot l^2/D$ (where l is the thickness of the subepithelial layer and D the Cl^- diffusion coefficient in this space). If l = 550 μm and D = $1.56 \cdot 10^{-5}$ cm^2sec^{-1} (equal to the free diffusion coefficient reduced by 23% for a tortuosity factor in the connective tissue; *see* Diamond, 1966 and Barry & Diamond, 1970), the half-time is found to be about 75 sec, in good agreement with $t_{1/2}$ of compartment A, under control conditions (61 sec) or of the sole compartment remaining under SCN^- treatment (94 sec). Conversely, it is quite different from $t_{1/2}$ of compartment B (5 min).

Third, the sweeping away effects, caused by 100 mM sucrose in the mucosal or in the serosal medium, should involve a decrease or an increase in the $^{36}Cl^-$ J_s/J_m ratio, respectively, as actually occurs. This is evidence that the experimental model is correctly responsive to external challenges.

Finally, the luminal addition of nystatin should mainly enhance $^{36}Cl^-$ J_m from the cellular compartment. Actually, J_m increases and the increased efflux should be of cellular origin, as nystatin has been added 4 min after the washout start, when the measured efflux is dominated by the cellular component. The observation of the effects caused by nystatin is particularly noteworthy, as this drug, e.g., in thin lipid membranes, induces the formation of pores through which ions (mainly anions), water and small nonelectrolytes can permeate (Cass, Finkelstein & Crespi, 1970; Holz & Finkelstein, 1970). Thus, its effects should be taken as a reference when observing the $^{36}Cl^-$ J_m modified by HCTZ, if it is true that HCTZ opens an apical Cl^- leak.

The HCTZ Effects on Cl^- Backflux

HCTZ (10^{-3} M) was shown to depolarize the apical membrane potential of the rabbit gallbladder epithelium

by about 3 mV (Cremaschi et al., 1992). Preliminary results indicate that the depolarization, elicited in a few seconds, reaches a maximum of 3 mV in 10 min, even with $2.5 \cdot 10^{-4}$ M HCTZ; it seems to be related to the opening of an apical, SITS-sensitive, Cl^- conductance (Cremaschi et al., 1993). Thus, $2.5 \cdot 10^{-4}$ M HCTZ has been used in the present study to examine the drug effects on the apical Cl^- efflux.

$^{36}Cl^-$ J_m increases on treatment and this directly reflects the action of HCTZ. However, based on the tracer flux alterations, the nonradioactive Cl^- backflux cannot be quantified exactly, inasmuch as the tissue steady-state has been perturbed. It is only possible to calculate that the total radioactivity, which has exited apically from the tissue, is 2.3 times higher upon treatment compared to that of the control.

The increase in $^{36}Cl^-$ J_m, elicited by HCTZ, may be ascribed to the cell-lumen (rather than to the subepithelium-lumen) $^{36}Cl^-$ efflux. In fact, 4 min after the start of the washout, when treatment begins, the radioactivity remaining in the tissue is dominated by the cellular component (70%) and the dominance increases with time to 100%. Moreover, the serosa-mucosa flux, which follows the same route of the subepithelium-lumen efflux, does not increase like J_m, but even decreases. Finally, the transepithelial diffusion potentials, which measure the ion selectivity of the paracellular pathway, are not affected by the drug. Thus, the paracellular conductance should decrease in a nonselective way, whereas $^{36}Cl^-$ J_m increases, and the increase is selective and SITS sensitive.

It is noteworthy that, compared to the control, HCTZ-SITS treatment maintains a higher efflux asymmetry at the end of the unloading when the epithelial component of J_m is the sole component remaining. This probably indicates that, after the closure of the HCTZ-elicited apical leak by SITS, the electroneutral Cl^- efflux to the lumen is unmasked and even reduced compared to the control. Such an observation is in agreement with inhibition by HCTZ, not only of the electroneutral influx (Cremaschi et al., 1992) but also of the electroneutral backflux, both mediated by the Na^+-Cl^- symporter, similarly to what was found by Stokes (1984, 1988) in the fish urinary bladder.[3]

As to why the SITS-sensitive Cl^- backflux is elicited by HCTZ in rabbit gallbladder but not in fish urinary bladder, only speculations are possible. First, SITS-sensitive Cl^- channels, opened by HCTZ, might be present in the gallbladder but not in the urinary bladder. Secondly, no Cl^-/HCO_3^- exchange has been observed in the urinary bladder (Stokes, 1984); by contrast, the exchanger is present in rabbit gallbladder, even if it is silent in the experimental conditions used in this work (Cremaschi et al., 1983, 1987*b*). It has been suggested by several authors that HCTZ is also able to inhibit the exchanger (Cousin & Motais, 1976; Ferriola, Acara & Duffey, 1986; Karnisky & Aronson, 1987; Stanton, 1988; Porta & Cremaschi, 1993). We can hypothesize that this inhibition is due to a large increase in the well-known inner basal Cl^- conductance present in the exchanger (Knauf, 1979; Rothstein & Ramjeesingh, 1980; Knauf, Law & Marchant, 1983; Frölich, Leibson & Gunn, 1983); this is in accordance with the SITS dependence of both the Cl^- backflux and conductance elicited by HCTZ.

This research was supported by the Ministry of University and Scientific and Technologic Research, Rome. We are much indebted to Prof. G. Meyer for careful reading and discussion of the manuscript, and to Dr. G. Bottà for many helpful suggestions.

References

Barry, P.H., Diamond, J.M. 1970. Junction potentials, electrode standard potentials and other problems in interpreting electrical properties of membranes. *J. Membrane Biol.* **3**:93–122

Cass, A., Finkelstein, A., Krespi, V. 1970. The ion permeability induced in thin lipid membranes by the polyene antibiotics nystatin and amphotericin B. *J. Gen. Physiol.* **56**:100–124

Costanzo, L.S., Windahger, E.E. 1978. Calcium and sodium transport by the distal convoluted tubule of the rat. *Am. J. Physiol.* **235**: F492–F506

Cousin, J.L., Motais, R. 1976. The role of carbonic anhydrase inhibitors on anion permeability onto ox red blood cells. *J. Physiol.* **256**:61–80

Cremaschi, D., Hénin, S. 1975. Na^+ and Cl^- transepithelial routes in rabbit gallbladder. Tracer analysis of the transports. *Pfluegers Arch.* **361**:33–41

Cremaschi, D., Hénin, S., Meyer, G. 1979. Stimulation by HCO_3^- of Na^+ transport in rabbit gallbladder. *J. Membrane Biol.* **47**:145–170

Cremaschi, D., Meyer, G. 1982. Amiloride-sensitive sodium channels in rabbit and guinea-pig gallbladder. *J. Physiol.* **326**:21–34

Cremaschi, D., Meyer, G., Bermano, S., Marcati, M. 1983. Different sodium chloride cotransport systems in the apical membrane of rabbit gallbladder epithelial cells. *J. Membrane Biol.* **73**:227–235

Cremaschi, D., Meyer, G., Bottà, G., Rossetti, C. 1987*a*. The nature of the neutral Na^+-Cl^- coupled entry at the apical membrane of the rabbit gallbladder epithelium: II. Na^+-Cl^- symport is independent of K^+. *J. Membrane Biol.* **95**:219–228

Cremaschi, D., Meyer, G., Rossetti, C., Bottà, G., Palestini, P. 1987*b*. The nature of the neutral Na^+-Cl^- coupled entry at the apical membrane of rabbit gallbladder epithelium: I. Na^+/H^+, Cl^-/HCO_3^- double exchange and Na^+-Cl^- symport. *J. Membrane Biol.* **95**: 209–218

[3] A hypothetical, basal and electroneutral, Cl^- backflux, occurring through the silent Cl^-/HCO_3^- exchange and inhibited by SITS, can be discarded as no SITS-sensitive component of Cl^- influx has been observed in phosphate saline (Cremaschi et al., 1987*b*). Likewise, no basal conductive Cl^- backflux inhibited by SITS can be hypothesized, inasmuch as no basal SITS-sensitive Cl^- conductance is present (Hénin & Cremaschi, 1975; Cremaschi & Meyer, 1982; Cremaschi et al., 1987*a*).

Cremaschi, D., Porta, C., Bottà, G., Meyer, G. 1992. Nature of the neutral Na^+-Cl^- coupled entry at the apical membrane of rabbit gallbladder epithelium: IV. Na^+/H^+, Cl^-/HCO_3^- double exchange, hydrochlorothiazide-sensitive Na^+-Cl^- symport and Na^+-K^+-$2Cl^-$ cotransport are all involved. *J. Membrane Biol.* **129:**221–235

Cremaschi, D., Porta, C., Bottà, G., Meyer, G. 1993. Hydrochlorothiazide inhibits NaCl symport and opens a Cl^- conductance in rabbit gallbladder. *Pfluegers Arch.* **423:**R10, 24 (*Abstr.*)

Diamond, J.M. 1966. A rapid method for determining voltage-concentration relations across membranes. *J. Physiol.* **183:**83–100

Duffey, M.E., Frizzell, R.A. 1984. Flounder urinary bladder: mechanism of inhibition by hydrochlorothiazide (HCT). *Fed. Proc.* **43:**932 (*Abstr.*)

Eveloff, J.L., Warnock, D.G. 1987. Activation of ion transport systems during cell volume regulation. *Am. J. Physiol.* **252:**F1–F10

Ferriola, P.C., Acara, M.A., Duffey, M.E. 1986. Thiazide diuretics inhibit Cl^- absorption by rabbit distal colon. *J. Pharmacol. Exp. Ther.* **238:**912–915

Frölich, O., Leibson, C., Gunn, R.B. 1983. Chloride net efflux from intact erythrocytes under slippage conditions. *J. Gen. Physiol.* **81:**127–152

Frömter, E., Diamond, J.M. 1972. Route of passive ion permeation in epithelia. *Nature New Biol.* **263:**5–13

Hénin, S., Cremaschi, D. 1975. Transcellular ion route in rabbit gallbladder. Electric properties of the epithelial cells. *Pfluegers Arch.* **355:**125–139

Hénin, S., Cremaschi, D., Schettino, T., Meyer, G., Lora Lomia Donin, C., Cotelli, F. 1977. Electrical parameters in gallbladder of different species. Their contribution to the origin of the transmural potential difference. *J. Membrane Biol.* **34:**73–91

Holz, R., Finkelstein, A. 1970. The water and nonelectrolyte permeability induced in thin lipid membranes by the polyene antibiotics nystatin and anphotericin B. *J. Gen. Physiol.* **56:**125–145

Jacquez, J.A. 1972. Compartmental analysis in biology and medicine: kinetics of distribution of tracer-labeled materials. Chapters 5–6. Elsevier Publishing, Amsterdam

Karniski, L.P., Aronson, P.S. 1987. Anion exchange pathways for chloride transport in rat renal microvillus membranes. *Am. J. Physiol.* **253:**F513–F521

Knauf, P.A. 1979. Erythrocyte anion exchange and the band 3 protein: transport kinetics and molecular structure. *Curr. Top. Membr. Trans.* **12:**249–363

Knauf, P.A., Law, F.Y., Marchant, P.J. 1983. Relationship of net chloride flow across the human erythrocyte membrane to the anion exchange mechanism. *J. Gen. Physiol.* **81:**95–126

Kotyk, A., Janacek, K. 1970. Cell Membrane Transports. Principles and Techniques. pp. 151–172, 240–245. Plenum, New York

Lippe, C., Bianchi, A., Cremaschi, D., Capraro, V. 1965. Different types of asymmetric distribution of hydrosoluble and liposoluble substances at the two sides of a mucosal intestinal preparation. *Arch. Int. Physiol. Bioch.* **73:**43–54

Meyer, G., Bottà, G., Rossetti, C., Cremaschi, D. 1990. The nature of the neutral Na^+-Cl^- coupled entry at the apical membrane of rabbit gallbladder epithelium: III. Analysis of transport on membrane vesicles. *J. Membrane Biol.* **118:**107–120

Porta, C., Cremaschi, D. 1993. Bicarbonate transport, double ion exchange and Na^+-Cl^- symport are all inhibited by hydrochlorothiazide in the apical membrane of the epithelium of rabbit gallbladder. *Rend. Fis. Acc. Lincei S9* **4:**179–185

Riccardi, D., Porta, C., Cremaschi, D. 1993. Sulphates and phosphates reduce the sensitivity to hydrochlorothiazide (HCTZ) of the transepithelial NaCl transport in rabbit gallbladder. *Rend. Fis. Acc. Lincei S9* **4:**187–192

Rothstein, A., Ramjeesingh, M. 1980. The functional arrangement of the anion channel of red blood cells. *Ann. NY Acad. Sci.* **358:**1–12

Stanton, B.A. 1988. Electroneutral NaCl transport by distal tubule: evidence for Na^+/H^+-Cl^-/HCO_3^- exchange. *Am. J. Physiol.* **254:** F80–F86

Stokes, J.B. 1984. Sodium chloride absorption by the urinary bladder of the winter flounder. A thiazide sensitive, electrically neutral transport system. *J. Clin. Invest.* **74:**7–16

Stokes, J.B. 1988. Passive NaCl transport in the flounder urinary bladder: predominance of a cellular pathway. *Am. J. Physiol.* **255:** F229–F236

Velasquez, H., Good, D.W., Wright, F.S. 1984. Mutual dependence of sodium and chloride absorption by renal distal tubule. *Am. J. Physiol.* **247:**F904–F911

Wedner, H.J., Diamond, J.M. 1969. Contribution of unstirred-layer effects to apparent electrokinetic phenomena in the gallbladder. *J. Membrane Biol.* **1:**92–108

Wright, E.M., Smulders, A.P., Tormey, J.McD. 1972. The role of the lateral intercellular spaces and solute polarization effects in the passive flow of water across the rabbit gallbladder. *J. Membrane Biol.* **7:**198–219

Appendix

Let us suppose that a tissue in steady-state, loaded with $^{36}Cl^-$, is made by only one compartment facing equal mucosal and serosal chambers. With the total $^{36}Cl^-$ efflux $-dq/dt$ and q the quantity of labeled substance in the compartment, the differential equation describing this efflux in relation to q is as follows (Lippe et al., 1965; Kotyk & Janacek, 1970):

$$-\frac{dq}{dt} = A(P_m + P_s)\frac{q}{V} \tag{A1}$$

where A is the total area useful for the efflux, P_m and P_s are the unloading constants at the mucosal and serosal faces of the compartment, V is the compartment volume. P_m and P_s are equal to Φ_m/C and Φ_s/C (that is to the nonradioactive steady fluxes from the compartment to the mucosal or serosal medium per area unity, divided by the nonradioactive Cl^- concentration in the compartment: Kotyk & Janacek, 1970); they are equivalent to permeability constants if the nonradioactive flux is described by Fick's law. Therefore, q at any instant t is:

$$q = q_o \cdot \exp\left|-\frac{A(P_m + P_s)}{V}t\right| \tag{A2}$$

where q_o is the quantity of the labeled substance in the compartment after loading at the beginning of the washout experiment (0 min time). By substituting q in Eq. (A1), the efflux becomes:

$$-\frac{dq}{dt} = A(P_m + P_s)C_o \cdot \exp\left|-\frac{A(P_m + P_s)}{V}t\right| \tag{A3}$$

where C_o is the concentration of the labeled substance at 0 min time. The single unidirectional effluxes exiting the compartment toward the mucosal or the serosal medium, expressed as rates of increase in radioactivity in the respective medium, per unity of the corresponding membrane area (J_m, J_s), are:

$$J_m = P_m C_o \cdot \exp\left|-\frac{A(P_m + P_s)}{V}t\right| \tag{A4}$$

$$J_s = P_s C_o \cdot \exp\left|-\frac{A(P_m + P_s)}{V}t\right| \tag{A5}$$

Since P_mC_o and P_sC_o are the two effluxes at $t = 0$ min (i.e., $J_{m,o}$ and $J_{s,o}$) and $A(P_m + P_s)/V$ is the rate constant of unloading from the compartment (i.e., k), one can write:

$$J_m = J_{m,o}\exp(-kt) \quad \text{(A6)}$$

$$J_s = J_{s,o}\exp(-kt) \quad \text{(A7)}$$

which, in semilogarithmic form, give the equations of two parallel straight lines

$$\log J_s = \log J_{s,o} - kt/2.3 \quad \text{(A8)}$$

$$\log J_m = \log J_{m,o} - kt/2.3 \quad \text{(A9)}$$

Moreover, from Eqs. (A4–A9) it is evident that k is predicted as being equal for the two effluxes so that

$$J_s/J_m = J_{s,o}/J_{m,o} = P_s/P_m = \Phi_s/\Phi_m \quad \text{(A10)}$$

at any instant. Therefore, the ratio is constant throughout the unloading period and equal to the ratio of the corresponding nonradioactive fluxes in steady-state.